ELSEVIER

Biophysical Chemistry 90 (2001) 279–299

Biophysical Chemistry

www.elsevier.nl/locate/bpc

Two types of urate binding sites on hemocyanin from the crayfish *Astacus leptodactylus*: an ITC study

N. Hellmann*, E. Jaenicke, H. Decker

Institute of Molecular Biophysics, Jakob Welder Weg 26, 55128 Mainz, Germany

Received 5 December 2000; received in revised form 2 March 2001; accepted 7 March 2001

Abstract

The oxygen binding behaviour of hemocyanins from Crustacea is regulated by small organic compounds such as urate and L-lactate. We investigated the binding characteristics of urate and the related compound caffeine to the 2×6-meric hemocyanin of *A. leptodactylus* under fully oxygenated conditions employing isothermal titration calorimetry (ITC). An analysis of urate and caffeine binding based on a model of n identical binding sites resulted in approximately four binding sites for caffeine and eight for urate. This result suggests that the binding process for these effectors is more complex than this most simple model. Therefore, we introduced a number of alternative models. Displacement experiments helped to select the appropriate model. Based on these experiments, at least two different types of binding sites for urate and caffeine exist on the 2×6-meric hemocyanin of *A. leptodactylus*. The two binding sites differ strongly in their specificity towards the two analogues. It can be hypothesized that two different subunit types (β and γ) are responsible for the two types of binding sites. © 2001 Published by Elsevier Science B.V.

Keywords: Urate; Cooperativity; Isothermal titration calorimetry; Allosteric interaction; Nesting model; Hemocyanin

1. Introduction

Hemocyanins are respiratory proteins found in the hemolymph of molluscs and arthropods [1–3]. While molluscan hemocyanins form cylindrical structures, arthropod hemocyanins are composed as multiples of hexamers, depending on the species (1×6, 2×6, 4×6, 6×8 and 8×6). Their oxygen binding behaviour is characterized by a strong cooperativity with Hill-coefficients up to 11, which are the highest reported for any protein [3–6]. The structures of hexamers from two different species were solved by X-ray crystallography [7–10]. The arthropod hexamer is built up by two trimers, which are assembled back to back in a slightly rotated manner [7]. An individual subunit consists of three domains with different fold-

* Corresponding author. Tel.: +49-6131-392-3565; fax: +49-6131-392-3557.

E-mail address: nadja@biophysik.biologie.uni-mainz.de (N. Hellmann).

PII: S0301-4622(01)00150-8

ing motifs. The first domain is dominated by α-helices. The second domain contains the four-α-helix-bundle carrying the binding site for oxygen. Oxygen can reversibly bind between two copper atoms in a peroxo- (μ–η^2–η^2) complex coordination [7]. A β-barrel forms the third domain. In crustaceans, only 1×6- and 2×6-mers were found. The relative orientation of the two hexamers to each other is very similar for various 2×6-meric crustacean hemocyanin as deduced from electron micrographs [11,12]. The oxygen binding behaviour of crustacean hemocyanin is modulated by various effectors: pH, urate, L-lactate [6,13–17], dopamine and related substances [18,19], and nitrogen metabolites, such as ammonium and trimethylamine [20]. In order to understand the allosteric mechanism in these complex hemocyanins, knowledge of the binding behaviour of the effectors is necessary.

The effect of protons and L-lactate on the oxygen binding of crustacean hemocyanins is well investigated [6,13,14,21–23]. Our study focuses on the natural effector urate and the chemically very similar compound caffeine. The effect of urate on the oxygen binding was investigated for several crustacean hemocyanins by several authors [13,15–18]. In all cases, urate shifted the p_{50} towards lower oxygen concentrations. This indicates that urate preferentially binds to the oxy-state. However, only few data for urate binding to hemocyanins are available. A stoichiometry of two urate molecules per hexamer and a binding constant of approximately 36 000 M^{-1} were reported for hemocyanin from *H. vulgaris* in the oxy-state based on dialysis experiments at 20°C [25]. In a more recent study the binding constant for urate was determined to 8500 M^{-1} at 20°C. The value was independent of pH in the range between 7.55 and 8.15. The stoichiometry of two per 2×6 mer was confirmed; however, the binding of caffeine to the two binding sites exhibited positive cooperativity [24].

We investigated the binding behaviour of urate and its analogue caffeine to the 2×6-meric crustacean hemocyanin of *A. leptodactylus* in the oxy-state. The structures of these molecules are included in Fig. 3. The hemocyanin of *A. leptodactylus* consist of two identical hexamers. Each hexamer contains four different subunit types (2β, 2γ, 1α and 1α′), which can be distinguished immunologically [12]. The two subunits α′ form a disulfide-bridge, which connects the two hexamers.

Applying isothermal titration calorimetry (ITC), we found that the binding of urate and caffeine can not be explained by a simple approach since the apparent stoichiometry for these ligands differs by a factor of two. A detailed analysis was performed by testing several models. In order to find the appropriate model displacement experiments between the two effectors were performed.

2. Experimental

2.1. Chemicals

Hemocyanin was purified from fresh hemolymph drawn from *A. leptodactylus* purchased from a local fish supplier. Hemolymph was centrifuged for 20 min to remove cellular debris. The supernatant was centrifuged for 6 h at 200 000 *g* at 4°C to obtain the hemocyanin as a pellet. The pellet was resuspended and applied to a size exclusion column (Fractogel TSK HW 55(S), diam 26 mm, length 100 cm) to separate hemocyanin 12-mer from other aggregation states and additional proteins. Hemocyanin was stored in 0.1 M Tris buffer containing 20 mM $CaCl_2$, 20 mM $MgCl_2$, 0.2 g l^{-1} azide (pH 8) at 4°C. All experiments were performed in the same buffer without azide and pH 7.5 at 15°C. Protein solutions were dialyzed against this buffer prior to the experiments and effector solutions were prepared from the dialysis buffer. Uric acid and caffeine were purchased from Sigma Chemicals (Deisenhofen). The concentration of hemocyanin was determined photometrically at 278 nm based on an extinction coefficient of 1.42 mg (ml cm)$^{-1}$ and a molecular weight of 994 000 Da based on light scattering experiments. Concentrations of effector solutions were also determined photometrically based on an extinction coefficient of 12 600 M^{-1} cm^{-1} at 293 nm for urate [26] and 9500 M^{-1} cm^{-1} at 272 nm for caffeine as determined experimentally by weighted amounts of caffeine.

2.2. Isothermal titration calorimetry

The experiments were performed with the MCS ITC from MicroCal (Northampton, MA, USA). A typical recording after baseline subtraction is shown in Fig. 1a. Aliquots of the effector (uric acid or caffeine, 1×2 μl, 25×10 μl) were injected into a cell with 1.356 ml of hemocyanin solution at 15°C. The time between two injections was shorter at the end in order to reduce duration of mechanical stress. Solutions of uric acid contained not more than 2 mM due to the limited solubility. Any rigorous stirring in order to accelerate solubilization was omitted when preparing the urate solution in order to avoid precipitation. The concentration of caffeine went up to 3.5 mM. The binding of ligand to the macromolecule is accompanied by a change in enthalpy, which leads to a small temperature difference between sample and reference cell. The electrical power needed to compensate this temperature difference is regulated by a feedback mechanism and provides the signal to monitor the binding process [27–29]. The corrections due to heats of dilution of protein and ligand were determined separately ('blank' experiments) and were rather small (see Fig. 1b). Typical values were approximately 24 μJ per 10 μl as a total. We estimated the error in the calculated heat per injected ligand after all corrections to 1.25 kJ mol^{-1}, based on the variations in the 'blank' measurements in different experiments. Measurements were performed with a stirring speed of the syringe of 200 rev. min^{-1} to avoid protein precipitation. The oxygen saturation of the hemocyanin after the experiments was checked by determining the absorption at 340 nm, including a correction for the absorption of the effector. The deviation of the measured value for the absorption from the value expected based on the concentrations was less than 3%. Thus, no influence of the measuring procedure on the hemocyanin saturation could be detected. Native PAGE of the protein solution before and after the experiment did not indicate dissociation of the 12mers due to the mechanical stress induced by stirring.

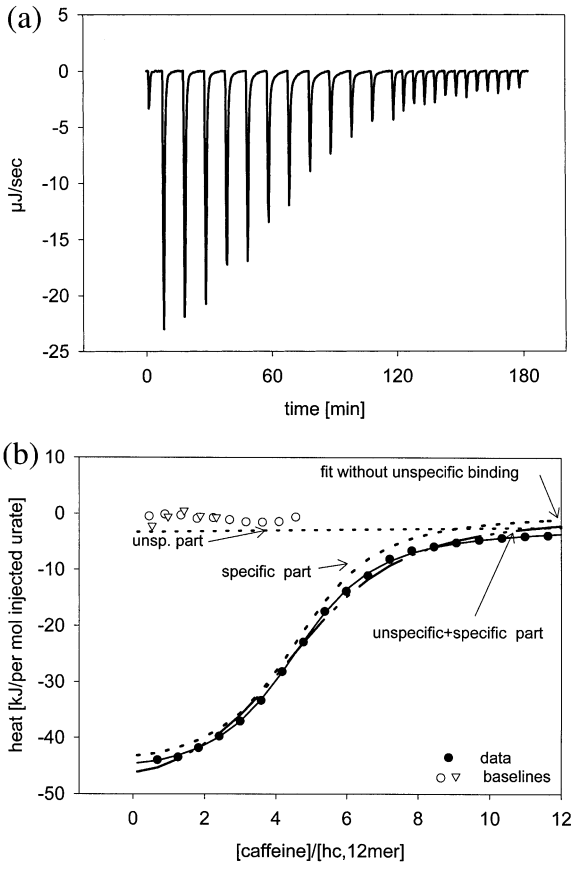

Fig. 1. Binding of caffeine. (a) Baseline-corrected tracing of 25 injections of caffeine into hemocyanin. (b) Corresponding integrated heats (closed symbols) together with dilution heats (open symbols). The binding curve was analyzed based on a model of *n* identical binding sites (thick broken line, fit a). In order to improve the agreement between data and calculated curve, a model including unspecific binding also was applied (solid line, fit b). The contribution of unspecific and specific binding for this analysis is drawn separately (dotted lines). The corresponding fit parameters (fit b) are given in Table 1, denoted by an asterisk.

2.3. Data analysis

The data analysis was performed based on different models. A model with n identical binding sites including unspecific binding was used employing the fitting routine of SigmaPlot. For models with two types of sites or interacting sites the fitting routine included in the ITC Software

(MicroCal Origin) was used. In addition, binding parameters for further models were deduced as presented below.

3. Models for effector binding

In a typical ITC-experiment, the effector is titrated stepwise into the solution. In order to derive the equation which is fitted to the ITC data, the change in enthalpy (ΔH_i) due to presence of effector compared to the situation in absence of effector has to be calculated for each titration step i. Then, the measured enthalpy change upon each titration step ΔH_{meas} is given by

$$\Delta H_{meas} = \Delta H_i - \Delta H_{i-1} \quad (1)$$

The expression for ΔH_{meas} has to be modified to include experimental artifacts such as solution displacement. These modifications were applied as recommended by the Microcal Tutorial (Northampton, MA, USA). At a given concentration of protein $[Hc]_o$ and effector x_{tot}, the enthalpy (H) at equilibrium is the sum of the enthalpies of all species present (free effector, free protein, effector–protein complexes). The enthalpy prior to the reaction (H_o) is the sum of enthalpies of the unreacted species $[Hc]_o$ and x_{tot}. The enthalpy change ΔH_i is determined by the difference $\Delta H_i = H - H_o$. If no other reactions than ligand binding occur, ΔH_i can be expressed entirely in terms of the number of bound effector molecules n_{bound} due to conservation of mass:

$$\Delta H_i = H - H_o = \Delta H^{\circ} n_{bound} = \Delta H_o V_o c_{bound} \quad (2)$$

where ΔH^{o} is the normalized reaction enthalpy for the binding reaction (J mol^{-1}). V_o denotes the reaction volume. If additionally effector-induced conformational changes occur, these have to be included as an extra term (see Appendix A). In all models presented the reaction enthalpy ΔH_i is expressed as a function of total protein concentration $[Hc]_o$ and free effector concentration x. It would be desirable to express ΔH_i as a function of total effector concentration. However, an analytical expression can be obtained only for the most simple models.

In order to interpret data obtained for urate and caffeine binding to *Astacus* hemocyanin, different binding models are introduced. In the following part, equations for the reaction enthalpy ΔH_i are given for these models. In this part, the equations are given for the presence of only one type of effector. In the appendix the more general form for the presence of both effectors urate and caffeine and the derivation of the equations are given.

3.1. Model 1: n identical binding sites including unspecific binding

The analysis of n identical binding sites characterized by K_{sp}, ΔH^{o}_{sp} and n according to Wiseman et al. [27] was extended to include also possible unspecific binding (K_{unsp}, ΔH^{o}_{unsp}) to improve the agreement between data and fit. The reaction enthalpy ΔH_i is given by the following equation:

$$\Delta H_i = \left[\Delta H^{o}_{sp} \frac{n K_{sp} x}{1 + K_{sp} x} + \Delta H^{o}_{unsp} K_{unsp} x \right] V_o [Hc]_o \quad (3)$$

In this particular case, x can be expressed as a function of total protein and effector concentration (see Appendix A).

The value of K_{unsp} had to be kept below 300 M^{-1} in order to maintain validity of the above approach, i.e. that the additional binding process can be regarded as unspecific binding. Furthermore, this value cannot be determined independently due to a strong numerical interdependence between ΔH_{unsp} and K_{unsp}. Therefore, $K_{unsp} = 10$ M^{-1} was set constant in all fitting routines when this model was applied (see Appendix A). The value of K_{unsp} determines the value obtained for ΔH_{unsp} in the fitting routine. For this approximation, the product $\Delta H_{unsp} K_{unsp}$ remains constant.

3.2. Model 2: stacking model

The analysis based on n identical binding sites yielded apparent stoichiometries for urate, which are approximately twice as high as for caffeine. One possibility to explain this result is that the effectors have a tendency to stack on the binding site or bind as preformed dimers. This idea is supported by a report about stacking of caffeine in water [30]. Therefore, a model based on stacking of two effectors on the binding site was applied.

In this case, the following species have to be considered: hemocyanin (Hc), hemocyanin + monomeric effector (Hcx_1), hemocyanin + dimeric effector (Hcx_2), effector monomers in solution (x_1) and effector dimers in solution (x_2). The corresponding binding equilibria and equilibrium constants are depicted in the following scheme:

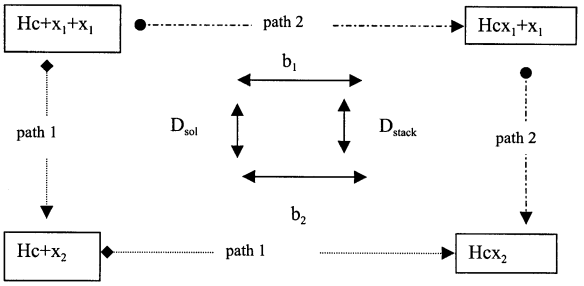

The stacking constants in solution and on the binding site are denoted by D_{sol} and D_{stack}, respectively. The binding constants for monomers and dimers to the binding sites are denoted by b_1 and b_2. If the dimers in solution and the dimers at the binding site have the same structure, the equilibrium constants given in the scheme are related to each other: $b_1 \times D_{stack} = b_2 \times D_{sol}$. The binding polynomial can be set up based on binding of monomers and dimers (path 1). In this case the stacking constant of the effector in solution has to be known to describe the concentration of free dimers. Alternatively, one can describe the binding as binding of monomers, on which a second effector can bind at the binding site (path 2). The latter approach is also applicable, if the dimers on the binding site have a different structure compared to the dimers in solution. Therefore, a binding polynomial according to path 2 was used. Furthermore, one may neglect the contribution of dimer formation to the observed binding enthalpy based on the following considerations: The stacking constant for the formation of caffeine dimers in water is approximately 60 M^{-1} [30]. Accordingly, at an effector concentration of 500 μM, approximately 5% of all caffeine molecules are present in the dimeric form. For urate, no such stacking in solution is reported, therefore the percentage of dimers is even less. Since the effector concentration in solution does not exceed 500 μM in our studies, the concentration of free monomers can be approximated by the total free effector concentration. The stacking model describes n identical binding sites, on which two effectors can bind stepwise. The expression for the reaction enthalpy is then given by

$$\Delta H_i = \left[\Delta H^{\circ}_{mon} \frac{b_1 x_1 + D_{stack} b_1 x_1^2}{1 + b_1 x_1 + D_{stack} b_1 x_1^2} + \Delta H^{\circ}_{dim} \frac{D_{stack} b_1 x_1^2}{1 + b_1 x_1 + D_{stack} b_1 x_1^2} \right] V_o n [Hc]_o \quad (4)$$

A scheme for the stacking on the binding sites is depicted in Fig. 2a. Since the above model is not included in the Origin analysis software package, we determined the values for b_1 and D_{stack} applying a trick: a suitable model provided by the software was fitted to the data and the parameters were reinterpreted in terms of the stacking model.

This suitable model was found in a model of two binding sites exhibiting cooperative binding with the microscopic binding constants K_1 and K_2, if the protein concentrations are multiplied by n prior to data analysis. The reaction enthalpy for this model is given by

$$\Delta H_i = \left[\Delta H^{\circ}_1 \frac{2K_1 x + K_2 K_1 x^2}{1 + 2K_1 x + K_2 K_1 x^2} + \Delta H^{\circ}_2 \frac{K_2 K_1 x^2}{1 + 2K_1 x + K_2 K_1 x^2} \right] V_o n [Hc]_o \quad (5)$$

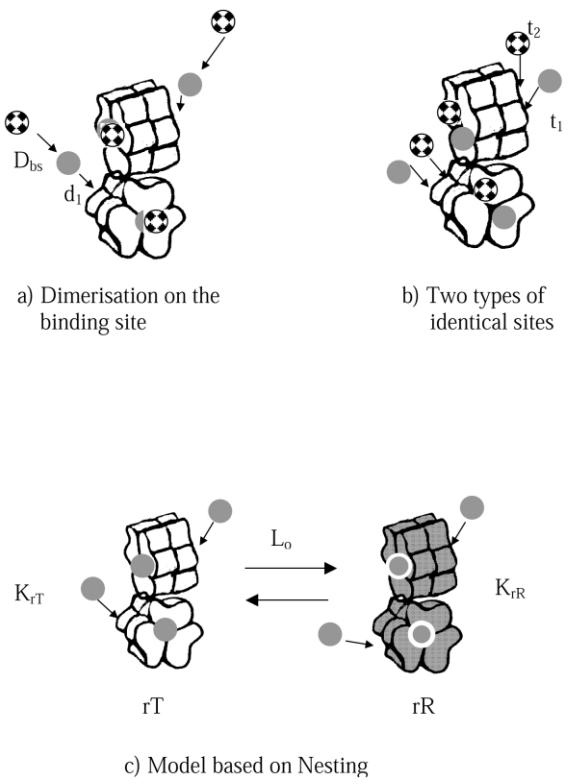

Fig. 2. three different models for effector binding to the 2×6-meric hemocyanin from *A. leptodactylus*. (a) A 2×6-mer with four binding sites. Two effector molecules bind successively on each binding site, with binding constants d_1 and D_{bs}. (b) A 12-mer which offers two types of binding sites for the effector. The two types of sites have different affinities (t_1, t_2) but the same number of binding sites ($n = 4$ each). (c) A scheme of an MWC-type model is depicted. Two conformations rR and rT are in equilibrium (L_o). In both conformations four binding sites are present. The affinity for the effector is given by the respective binding constants k_{rT} and k_{rR}.

For details see Appendix A (model 5). The interacting site model can also be used to describe a situation, where pairs of binding sites are located closely, so that binding of the first effector molecule to one binding sites influences the binding of the second.

Thus, for the stacking model and the interacting sites model the same functional relationship between ΔH_i and x, $[Hc]_o$ is found [Eqs. (4) and (5)]. The parameters for the two models may be related as follows:

$$2K_1 = b_1$$

$$K_2/2 = D_{stack}$$

$$\Delta H_1^o = \Delta H_{mon}^o$$

$$\Delta H_2^o = \Delta H_{stack}^o$$

This shows, that formally the stacking model is identical to a model for sequential binding to four cooperative dimers. Therefore, the thermodynamic constants for the stacking model can be obtained from fitting the parameters of an interacting site model to the data and re-interpretation of the fitted parameters.

Structurally, these two models differ from each other. The stacking model is based on four binding sites per 12-meric hemocyanin. In contrast, the interacting sites model is based on eight binding sites per 12-mer (four cooperative pairs of binding sites). There is no possibility to distinguish these two models based on binding curves for one type of effector. However, as will be shown later, displacement experiments allows to identify the more appropriate model.

3.3. Model 3: two types of binding sites

An alternative model considers two types of independent binding sites. Since we found approximately eight apparent binding sites for urate and approximately four for caffeine, we assumed that the 2×6-mers have two types of independent binding sites and each of the two types consists of four identical binding sites. Binding to the two different sites is characterized by two binding constants, t_1 and t_2. A scheme of this model is shown in Fig. 2b. The change in enthalpy upon binding is represented by

$$\Delta H_i = \left[\Delta H_1^o \frac{t_1 x}{1 + t_1 x} + \Delta H_2^o \frac{t_2 x}{1 + t_2 x} \right] V_o n [Hc]_o \tag{6}$$

The parameters for this model were determined using the MicroCal analysis package for two types of sites, setting the stoichiometry to $n = 4$ for both types.

3.4. Model 4: nesting model

No cooperative binding behaviour with respect to urate and caffeine was assumed in the models discussed so far. This seems to be in accordance with the individual effector binding curves which do not display any cooperativity. However, hemocyanins bind oxygen highly cooperatively. For a number of hemocyanins the complex cooperative binding behaviour has been well described by a hierarchical extension of the MWC-model, the nesting model [5,6]. In this section the nesting model is modified to describe effector binding under fully oxygenated conditions. With this model it is possible to account for the different apparent stoichiometries found for urate and caffeine. It can be shown that weak cooperativity in effector binding might yield apparently non-cooperative binding curves in an ITC experiment. The foot-print of cooperativity in such a case is an analogue-dependent stoichiometry.

In the nesting model, the half-molecule, a hexamer, represents the smallest allosteric unit. In addition, the entire hemocyanin molecule (2×6-mer) can also adopt two different conformations. These four possible conformations for each hexamer are characterized by particular affinity constants. Due to the hierarchical structure the four conformations cannot be combined arbitrarily. The possible conformations of the hexamer are determined by the conformation of the large allosteric unit, the 2×6-mer. In total, two conformations with high oxygen affinity exist. In contrast to the MWC-model, the simultaneous existence of two conformations is possible even when the hemocyanin is fully oxygenated. Therefore, a cooperative binding behaviour with respect to effector molecules is possible even under these conditions. The four conformations in the Nesting model are denoted by the indices tT, rT, tR, rR. Binding of oxygen (u) and effector (x) is described by the corresponding binding constants, $z_{\alpha\beta}$ and $k_{\alpha\beta}$, respectively, where $\alpha\beta$ indicates the conformation. The equilibrium between these conformations is given by three allosteric equilibrium constants L, l_{T} and l_{R}.

A direct fit of this model to the data was not attempted due to the large number of parameters and numerical difficulties. Instead, appropriate curves were simulated in order to evaluate whether weak positive cooperativity in effector binding could lead to the observed binding behaviour for urate and caffeine binding. A minimum of four binding sites for the entire 2×6-mer has to be assumed based on the analysis of urate and caffeine binding curves as discussed above. Therefore we assumed four effector binding sites per 2×6-mer. Since the experiments were performed under fully oxygenated conditions, only two of the four conformations (those with high oxygen affinity) are present in significant amounts. Therefore, the reaction enthalpy for effector binding is given by an equation which contains only these two conformations (rR, rT) (see Appendix A for details):

$$\Delta H_i = \left[\left(n\Delta H_{\mathrm{rR}}^{\mathrm{o,u}} + \Delta H_{\mathrm{conf}}\frac{L_{\mathrm{o}}}{1+L_{\mathrm{o}}}\right)K_{\mathrm{rR}}x_{\mathrm{u}}Q_{\mathrm{rR}}^{n-1} + \left(L_{\mathrm{o}}n\Delta H_{\mathrm{rT}}^{\mathrm{o,u}} - \Delta H_{\mathrm{conf}}\frac{L_{\mathrm{o}}}{1+L_{\mathrm{o}}}\right)K_{rR}x_{u}Q_{rT}^{n-1} + \Delta H_{\mathrm{conf}}\frac{L_{\mathrm{o}}}{1+L_{\mathrm{o}}}(Q_{\mathrm{rR}}^{n-1}-Q_{\mathrm{rT}}^{n-1})\right]\frac{[\mathrm{Hc}]_{\mathrm{o}}V_{\mathrm{o}}}{P(L_{\mathrm{o}})} \tag{7}$$

where $\alpha\beta = \mathrm{rR}, \mathrm{rT}$; $L_{\mathrm{o}} = L\dfrac{P_{rT}^{12}}{P_{rR}^{12}}$; $Q_{\alpha\beta} = 1 + K_{\alpha\beta}x$ is binding of effector x; and $P_{\alpha\beta} = 1 + z_{\alpha\beta}u$ is binding of oxygen u.

Here, the value of ΔH_{conf} corresponds to the enthalpy-difference between the rR- and the rT-conformations of the fully oxygenated, 12meric hemocyanin molecule.

For the simulations of binding data, starting values for k_{rR}, k_{rT} and L_{o} were chosen based on the binding constants found in the other models. In this procedure we tried to keep the value for L_{o} and the differences between the two values k_{rR}, k_{rT} as small as possible in order to keep cooperativity low. Based on the equations for c_{rR}, c_{tR}, M_{rR} and obeying mass conservation, the concentration of free effector was calculated numerically. Then, the concentration of bound effector and the concentration of hemocyanin in the conformation rR was calculated. In the next step, the

binding enthalpies were fitted to the data based on Eq. (A7). If the agreement between data and calculated curve was not satisfactory, the values for k_{rR}, k_{rT} and L_o were modified, and the procedure repeated. A scheme of this model is shown in Fig. 2c.

4. Results

Binding of urate and caffeine to the 2×6-meric hemocyanin from *A. leptodactylus* was investigated under conditions where the hemocyanin is fully oxygenated. The binding curves were analysed according to different models as described above. Neither for caffeine nor for urate indications of cooperativity were observed in the individual binding curves. Therefore, binding curves were analyzed assuming that n identical binding sites per 2×6-mers exist. However, as the fit did not agree perfectly with the data, we also allowed unspecific binding as shown for the caffeine binding in Fig. 1b (model 1). Obviously, the calculated curves obtained for a fit including unspecific binding is in better agreement with the experimental data. This was the case for all effector binding curves. For this model, each binding curve was analyzed individually. The averages of two experiments for each effector correspond to the results obtained when each pair is fitted simultaneously. The experimental data and the fitted curves together with the results for other models are shown in Fig. 3. The results for the analysis including unspecific binding are summarized in Table 1. Urate binding is characterized by approximately 7.8 ± 0.5 identical binding sites, with a binding constant of approximately $(67 \pm 12) \times 10^3$ M^{-1} and a binding enthalpy of -53.2 ± 2.5 kJ mol^{-1} (averages of two experiments). In contrast, caffeine binding involves only 4.3 ± 0.4 binding sites with a similar binding constant of approximately $(74 \pm 15) \times 10^3$ M^{-1}, and a lower binding enthalpy of -43.5 ± 0.4 kJ mol^{-1}. The observed large difference in stoichiometry for urate and caffeine by a factor of two is rather unexpected. Since the two compounds are chemical analogues one would expect the same number of binding sites, but different binding affinities and binding enthalpies. We considered this unexpected finding as a strong indication that the binding mechanism is more complex than first assumed. In order to find an appropriate mechanism, different possibilities were tested for applicability.

4.1. Interacting sites

The differences in stoichiometry for urate and caffeine binding might result from sterical inter-

Table 1
Parameters for n identical binding sites[a]

	Hc-conc (μM)	n	K_{sp} (M^{-1})	ΔH^o_{sp} (kJ mol^{-1})	$\Delta H^o_{unsp}/100$ (kJ mol^{-1})
Urate	13.1	8.3	79 000	−50.7	−36.8
	17.5	7.3	55 000	−55.3	95.0
Average		7.8	67 000	−53.2	–
Caffeine	39.2	4.6	88 000	−43.5	−90.4
	45.5*	3.9	59 000	−43.1	−86.7
Average		4.3	74 000	−43.5	–

[a] The binding curves obtained at different hemocyanin concentrations (Hc-conc) were analyzed assuming n identical binding sites and unspecific binding. The binding constant for unspecific binding was set constant at a value of 10 M^{-1}. The values for binding enthalpy for unspecific binding in the last column depend on the value chosen for K_{unsp}: $K_{unsp} \times \Delta H_{unsp} \approx$ constant. Therefore, the value is not well determined. The errors are as given in the fitting routine. Typical values are: 5% for K_{sp}, 1% for n, 3% for ΔH_{sp} and 8% for ΔH_{unsp}. However, the error in n is in fact larger due to the uncertainty in the molar extinction coefficient for hemocyanin. Data and calculated curve for the data set denoted with an asterisk are depicted in Fig. 1.

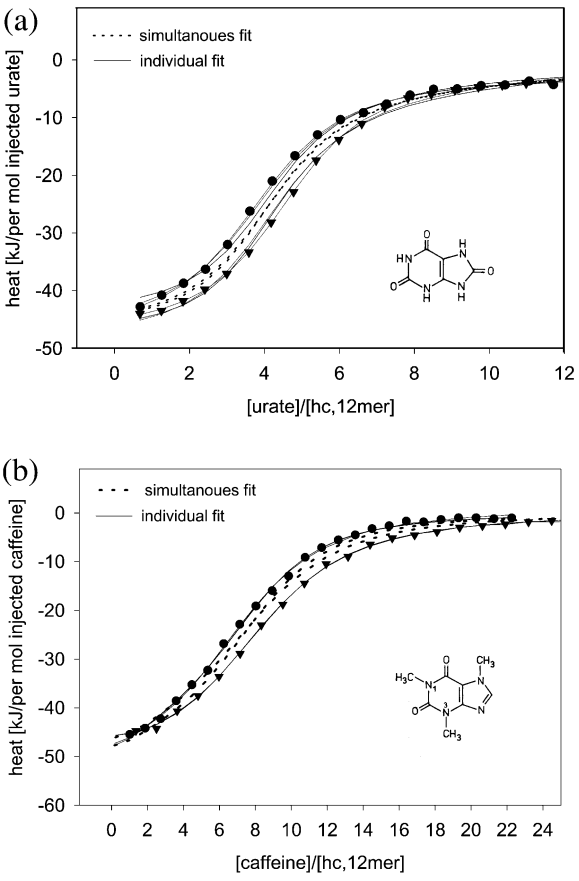

Fig. 3. Comparison of models for caffeine and urate binding. For each effector two sets of data at different hemocyanin concentrations (closed symbols) are shown. The fit results for each individual curve based on three models (model 1–3) are not distinguishable (solid lines). The parameters for model 1 is given in Table 1. When both sets for a given effector are fitted simultaneously, the calculated curve lies between both data sets (dotted). As an example, the result of a simultaneous fit for the stacking model is shown. The results for the other two models would not be distinguishable and are therefore omitted in the plot. The resulting parameters for the simultaneous fits are given in Table 2. The structure of the respective effectors is also shown.

actions between two sites. If pairs of binding sites are in close proximity, the binding of effectors to the first site of the pair might influence binding to the second binding site, yielding cooperative binding behaviour (model 5). The results of the data analysis indicate that for such a situation urate binding shows slightly positive cooperativity ($K_1 = 63\,000\ M^{-1}$, $K_2 = 77\,600\ M^{-1}$), whereas caffeine binding displays negative cooperativity ($K_1 = 63\,000\ M^{-1}$, $K_2 = 5900\ M^{-1}$).

4.2. Stacking model

When n identical binding sites are assumed, caffeine binding curves can well be described by approximately four identical binding sites. In contrast, urate binding seems to involve approximately eight binding sites per 2×6-mer as shown above. A possible explanation for this behaviour is, that four binding sites with identical or very similar binding affinity exist. But, once a binding site is occupied by an effector molecule, a second one can bind on top of it. The second binding process can be regarded as stacking on the binding sites. When the effector is bound to a binding site of a protein the tendency to stack might be strengthened or weakened compared to the situation in solution. This will depend on the chemical environment at the binding site. The parameters describing these two steps are the binding constants for the monomeric effector molecules b_1 and binding constants for the second monomer, D_{stack}, which describes the stacking process at the binding site (model 2; Fig. 2a). The values for these two parameters and the corresponding standard reaction enthalpies were determined by reinterpretation of the values obtained from the analysis based on interacting dimers (Table 2). This model can describe the data equally well as the model before. When each data set is analysed individually, the resulting curves are very close to the curves based on model 1 (data not shown). For further discussion, we refer to the value obtained by a simultaneous fit of each pair of binding curves. A high binding constant ($126\,000\ M^{-1}$) for the first urate molecule per binding site is found. Stacking, that is binding of the second effector molecule, occurs with a lower affinity of $39\,000\ M^{-1}$. In the case of caffeine binding, binding of the first effector molecule occurs with the same affinity as for urate, however, the second molecule is bound with a very low affinity of $3000\ M^{-1}$.

Table 2
Binding parameters obtained for models 2, 3 and 5 (see Fig. 2)[a]

Model		(M^{-1})	(kJ mol^{-1})	(M^{-1})	(kJ mol^{-1})
Interacting		K_1	ΔH^o_1	K_2	ΔH^o_2
Sites	Urate	$(63 \pm 0.2) \times 10^3$	-53.2 ± 1.3	$(77.6 \pm 0.3) \times 10^3$	-44.8 ± 1.7
	Caffeine	$(63 \pm 0.2) \times 10^3$	-46.1 ± 0.4	$(5.9 \pm 0.2) \times 10^3$	-22.6 ± 0.8
Stacking (model 2)		b_1	ΔH^o_{mon}	D_{stack}	ΔH^o_{stack}
	Urate	$(126 \pm 0.4) \times 10^3$	-53.2 ± 13	$(39 \pm 0.2) \times 10^3$	-44.8 ± 1.7
	Caffeine	$(126 \pm 0.4) \times 10^3$	-46.0 ± 0.4	$(2.5 \pm 0.1) \times 10^3$	-22.6 ± 0.8
Two types of		t_1	ΔH^o_{t1}	t_2	ΔH^o_{t2}
binding sites	Urate	$(119 \pm 29) \times 10^3$	-52.7 ± 2.1	$(52.4 \pm 8.8) \times 10^3$	-46.0 (fix)
(model 3)	Caffeine	$(133 \pm 40) \times 10^3$	-46.0 ± 0.4	$(3.0 \pm 1.5) \times 10^3$	-23.0 ± 5.9

[a] The parameters for the stacking model were obtained by re-interpretation of the binding parameters of the interacting sites model (see binding models). The binding parameters of the interacting sites model and the models for two types of binding sites were obtained by employing the software from MicroCal. The values are obtained from a simultaneous fit of two binding curves. The errors are as given by the fitting routine.

4.3. Two types of four identical binding sites

The assumption of different types of independent binding sites may also be a suitable model. A model where two types of binding sites exist, each with four binding sites, seems plausible based on the analysis as shown before. The curve calculated for this model also agrees well with the data (Fig. 3a,b). In Table 2 the results for this model are summarized. For both effectors, the two types of binding sites can be considered as a high affinity and a low affinity site. The high affinity sites for each of the effectors have similar affinities (119 000 M^{-1} and 132 000 mM^{-1}), whereas the low affinity sites are different (52 000 M^{-1} for urate and 3000 M^{-1} for caffeine). Thus, in contrast to urate, caffeine is bound with a very low binding constant to the second binding site. The results obtained for caffeine based on this model are comparable with the results when applying a model of *n* identical sites plus unspecific binding.

4.4. Nesting model

For other hemocyanins it has been reported that binding of ligands and effectors such as protons can well be described by the nesting model [5,6]. Therefore, we tried to apply this model as well. Our hypothesis was that the differences in stoichiometry for the two effectors result from a binding process with very low cooperativity, so that the individual binding curves do not appear to be cooperative. Although the nesting model assumes four different conformations, under fully oxygenated conditions only two of them have to be considered. So the binding process simplifies to a MWC-type model (see Appendix A) and the urate and caffeine binding is characterized by two binding constants each (K_{rR}, K_{rT}). As discussed in the Appendix A, binding curves were simulated based on an iterative process with preset values for K_{rT}, K_{rR} and L_o and the values for ΔH^o_{rR} and ΔH^o_{rT} were fitted to the data. The value for ΔH^o_{conf} was also kept at a preset value, since the values for ΔH^o_{rR} and ΔH^o_{conf} are highly correlated in the fitting process. The parameters given in Table 3 correspond to the best agreement between data and simulations we could achieve. For each effector, the two binding curves were simulated individually (Fig. 4). All four binding curves can be described with the same values for the allosteric equilibrium constant L_o, binding constants for oxygen z_{rR} and z_{rT} and standard reaction enthalpy for the conformational transition ΔH^o_{conf}. The value of 20 for $L_o = [rR_o]/[rT_o]$ indicates, that in absence of effector $[L_o/(1 +$

L_o)] = 95% of the molecules exist in the rT conformation. Both effectors prefer to bind to the rR conformation. However, the difference in affinities is larger for urate (70 000 and 15 000 M^{-1}) than for caffeine (50 000 and 30 000 M^{-1}). Therefore, increasing amounts of urate shift the conformational distribution towards rR, whereas increasing amounts of caffeine do this only to a small extent. At saturating concentrations of effectors, a new distribution of conformations is achieved. For urate, the fraction of molecules in the rT conformation is 81%, whereas for caffeine it is 92%. Thus, upon effector binding the conformational distribution is much less shifted in the case of caffeine compared to urate. However, even for urate the shift of 14% (from 95 to 81%) is not large. This explains why no cooperativity can be detected in the shape of the binding curves. The binding enthalpies differ somewhat for the two binding curves obtained for each effector (Table 3). However, for urate the differences are small (10% for ΔH_{rR}, none for ΔH_{rT}). For caffeine, the differences are larger (17% for ΔH_{rT}, approx. 50% for ΔH_{rR}). The binding constants and enthalpies indicate that the binding sites have similar thermodynamic characteristics for urate and caffeine binding in the rR conformation. However, in the rT conformation, the binding constants differ by a factor of two, the binding enthalpy by a factor of 2.5.

The results show that binding of urate and caffeine to oxy-hemocyanin can be described as a process with low cooperativity in terms of the nesting model. In this model, the stoichiometry is four per 2×6-mer. Possible locations for the binding sites would be the top and the bottom of each hexamer along the threefold axis (Fig. 2c).

In contrast to the models discussed so far, the nesting model could also account for the apparent influence of protein concentration on the binding parameters. In ITC experiments, protein concentration always has an influence on the sigmoidicity of the measured binding curve. However, when these curves are analyzed, the binding parameters are independent on the protein concentration as long as no additional process such as ligand induced aggregation occurs. In case of urate and caffeine binding to hemocyanin, the values of the parameters obtained for the model of n independent types of binding sites seem to depend slightly on protein concentration (Table 1). However, as is shown in Fig. 4, this dependence might be just the consequence of choosing the wrong model. The observation of the apparent dependence of the fit results on protein concentration in this case is entirely numerical and therefore artificial. This behaviour is confirmed by simulations performed for a MWC model as demonstrated in Fig. 5. Here, simulations for a MWC model for four binding sites exhibiting low cooperativity were performed for three different protein concentrations. The simulated curves were analyzed based on a model of n identical binding sites. The stoichiometry in all three cases is well below the value of 4. If the stoichiometry is fixed to a value of 4, no satisfactory agreement between fit and data can be achieved. This is demonstrated in Fig. 5 for the curve simulated for 20 μM hemocyanin. Thus, an analysis based on this simple model results in non-integer values for the

Table 3
Parameters obtained by the simulation of binding curves based on the nesting model[a]

Urate K_{rR} = 70 000 K_{rT} = 15 000 (M^{-1})			Caffeine K_{rR} = 50 000 K_{rT} = 30 000 (M^{-1})		
Hc-conc (μM)	ΔH^o_{rR} (kJ mol^{-1})	ΔH^o_{rT} (kJ mol^{-1})	Hc-conc (μM)	ΔH^o_{rR} (kJ mol^{-1})	ΔH^o_{rT} (kJ mol^{-1})
13.0	−239	−155	39.2	−186	−56.5
17.3	−213	−155	45.5	−130	−66.1

[a] The allosteric equilibrium constant was $L_o = [rT]/[rR] = 20$, the reaction enthalpy for the conformational transition ΔH_{conf} = 502 kJ mol^{-1} per 2×6-mer. Binding enthalpies for effector binding are given per binding site.

stoichiometry. The binding constant drops with increasing protein concentration whereas the apparent binding enthalpy slightly increases. Thus, under these conditions the dependence of the parameters on the protein concentration is the only indication that the simple model of *n*-identical binding sites is not appropriate.

4.5. Displacement experiments

All models discussed above describe the binding of urate and caffeine equally well. In order to distinguish between the models, displacement experiments were performed. In a first experiment aliquots of urate were injected into a solution containing hemocyanin and caffeine. In a second experiment, aliquots of caffeine were injected into a solution containing hemocyanin and urate (Fig. 6). The experimental binding curves are similar to the data obtained for binding of each effector individually: the shape suggests nothing more complicated than binding to n identical binding sites. The binding process and displacement of the effector present already has to be described

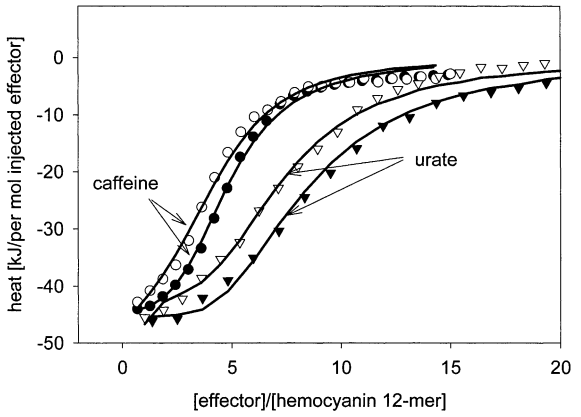

Fig. 4. Simulation of binding curves based on the nested MWC model. Binding curves at lower hemocyanin concentrations are depicted by open symbols [13 μM (urate), 39 μM (caffeine), whereas the closed symbols denote the higher concentrations (17 μM (urate), 45 μM (caffeine)]. For each binding set simulations were performed, in order to describe the binding behaviour based on the Nesting model. The binding parameters on which the simulations are based are shown in Table 3.

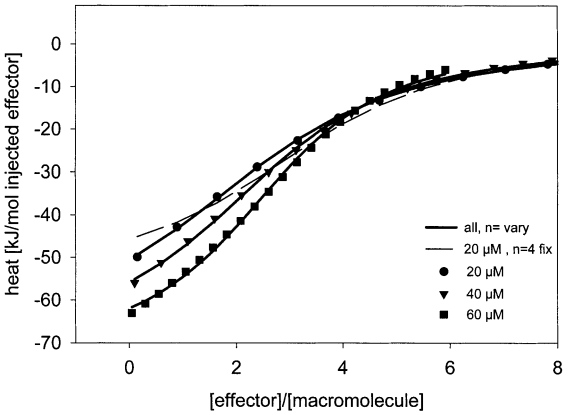

Fig. 5. Concentration dependence of binding curves for the nesting model. Based on the MWC-like model binding curves for a given set of binding parameters were calculated for different protein concentrations. The resulting curves were fitted based on a model assuming n identical binding sites. Closed symbols denote binding curves calculated for the nesting model. The binding parameter for effector were $k_{rR} = 50\,000\ M^{-1}$, $k_{rT} = 40\,000\ M^{-1}$, $L = 20$, $\Delta H^{o}_{conf} = 335\ kJ\ mol^{-1}$ (per macromolecule), $\Delta H^{o}_{rR} - 62.8\ kJ\ mol^{-1}$ (per binding site), $\Delta H^{o}_{rT} - 83.7\ kJ\ mol^{-1}$ (per binding site). The solid lines indicate calculated curves based on a fit assuming n identical binding sites. The values for the fitted parameters were: $n = 3.2$ for all concentrations; K dropped from $50\,000\ M^{-1}$ to $34\,000\ M^{-1}$ with increasing Hc-concentration and ΔH^{o} increased slightly from -69.5 to $-72.0\ kJ\ mol^{-1}$, respectively. The dotted line shows a fit obtained for the curve with 20 μM when $n = 4$ is set constant in the fitting routine.

by the corresponding binding constants and binding enthalpies for each of the models discussed so far. Since these are too many parameters to be determined to some accuracy based on such an experimental binding curve, we used the following approach to interpret the data: we predicted the binding curves for the displacement experiments based on the parameters obtained for the individual binding curves and compared these curves to the data. For each model the binding parameters were used as given in Table 2.

The application of the different models to displacement data is performed under the following assumptions: (1) no mixed dimers were included for the simulations of the stacking model and the interacting sites model; (2) two possibilities have to be distinguished for the simulation of two types of binding sites: (i) the high affinity sites for

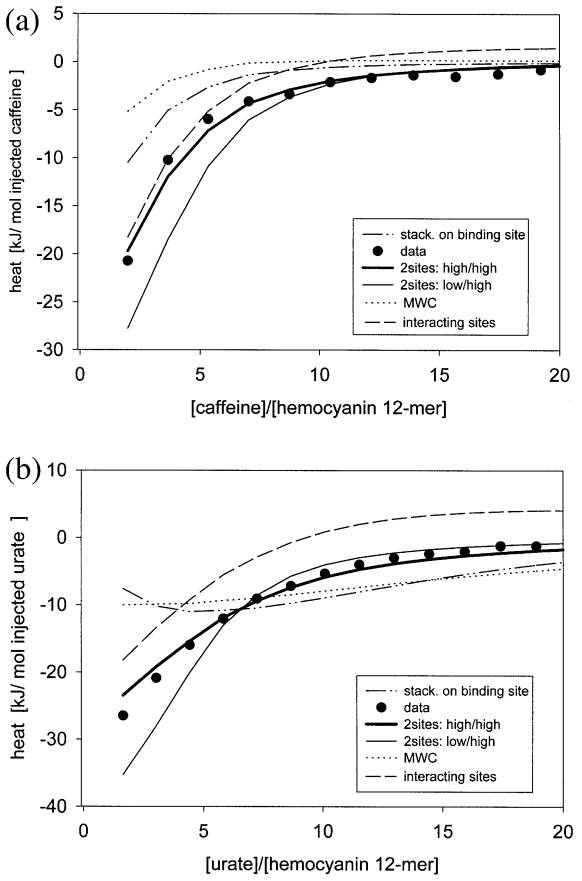

Fig. 6. Displacement experiments. Data (closed symbols) for titration of caffeine into 0.063 mM urate and 13 μM hemocyanin (a) and urate into 0.16 mM caffeine and 13 μM hemocyanin (b) are compared with the predictions based on different models. The best agreement is found for two sets of binding sites, where the high affinity sites for urate correspond to the high affinity sites of caffeine (thick solid line). The prediction for the nesting model and stacking on the binding site differ largely significantly.

caffeine may correspond to the high affinity sites for urate; or (ii) the high affinity sites for caffeine may correspond to the low affinity sites of urate.

A comparison of simulated curves and experimental data revealed that the only model that is consistent with the data, is a model assuming two types of identical binding sites (Fig. 6a,b). Furthermore, the high affinity site for caffeine corresponds to the high affinity for urate. Both the nesting model and the stacking model display a completely different shape of the displacement binding curves and can therefore be excluded.

5. Discussion

The oxygen binding behaviour of hemocyanins from crustaceans is modulated by the metabolic effector urate. Urate concentration is increased in vivo when oxygen availability is reduced [31]. This modulation was shown for *C. maenas* [16], *A. pallipedes* [17], *H. americanus* [25] and *A. leptodactylus* [18]. Increasing urate concentrations shift the p_{50} of oxygen binding curves towards lower values, indicating that urate binds preferentially to conformations with a high oxygen affinity. The structure of the active site, which define the oxygen affinity, must therefore be connected to the binding site of the effector. In order to understand the mechanism that is involved in this signal transduction process, the stoichiometry has to be determined and should be interpreted in terms of structural aspects. Furthermore, specificity of binding with respect to the molecular structure of the effector yields information about possible interactions involved in effector binding.

Crustacean hemocyanin is composed as a $2\times$ 6-mer. Each hexamer can be regarded as a dimer of two planar trimers, establishing a threefold symmetry axis. An efficient way to stabilize a certain conformation of these hemocyanins could be binding of an effector to the symmetry axis. This concept is for example realized in binding of one 2,3-DPG molecule per tetrameric hemoglobin [32]. However, in the case of hemocyanin from *A. leptodactylus*, our study revealed approximately eight binding sites for urate based on a simple analysis considering n identical sites. However, binding of a chemically similar reagent, caffeine, can be explained by the existence of only four identical binding sites. Thus, alternative models were considered to describe this unexpected difference in stoichiometry.

The following alternative models were tested: stacking of two effector molecules at the binding site (model 2), two types of four identical binding sites (model 3) weak cooperativity on the effector binding on the basis of the nesting model (model

4) and interacting sites (model 5). The stacking model is based on four binding sites per 2×6-mer, but a maximum of eight effector molecules can be bound due to stacking. The model considering two types of sites is based on eight binding sites per 2×6-mer, while the nesting model predicts four binding sites. The interacting sites model is based on eight binding sites. Since all models are in agreement with binding data for urate and caffeine, displacement experiments were performed to distinguish between the models. Based on the parameters obtained from the analysis of the binding curves for each of the two effectors alone, the binding curve for each of the effectors in the presence of the other was calculated for each model. A comparison of these with the experimental data revealed, that only one model, which considers two types of four identical binding sites, is consistent with the data. The two binding constants for urate are 119 000 M^{-1} ($K_{diss} = 8.4$ μM) and 52 000 M^{-1} ($K_{diss} = 19$ μM) with binding enthalpies and entropies of -52.7 and -46.0 kJ mol^{-1} (ΔH^o) and -87.9 and -71.2 J mol^{-1} K^{-1} (ΔS^o). For caffeine, the binding constants are 133 000 M^{-1} ($\Delta H^o = -46.0$ kJ mol^{-1}, $\Delta S^o = -62.8$ J mol^{-1} K) and 3000 M^{-1} ($\Delta H^o = -23.0$ kJ mol^{-1}, $\Delta S^o = +14.6$ J mol^{-1} K^{-1}).

This analysis shows that it is not necessary to assume different conformations in the oxy-state for this hemocyanin in order to explain the effector binding experiments. It is not clear whether both types of binding sites are of importance for allosteric regulation. However, if this were the case, the presence of two binding sites with different affinities would allow a sophisticated regulation of the conformational distribution even in an MWC model. In an MWC model only two conformations are assumed, denoted by R and T. The relative amount of both conformations is determined by the allosteric equilibrium constant L. The value of L is modulated by binding of effector according to the binding polynomials of the effectors:

$$L_{eff} = L_o \frac{Q_R}{Q_T}$$

If both binding polynomials Q_R and Q_T are of the form $(1 + kx)^n$, L_{eff} will change monotonously with the effector concentration. However, if the binding polynomials are of the form $(1 + k_1 x)^{n1}(1 + k_2 x)^{n2}$, a non-monotonous behaviour of L_{eff} in response to the effector concentration can be achieved when the two binding constants for each conformation have appropriate values. Thus, the relative amount of the two conformations also shift non-monotonously. This can add a new quality to the regulation process. However, the physiological importance remains to be elucidated.

The location of the eight binding sites in the 12-meric hemocyanin can only be hypothesized. Our results might indicate, that binding of urate occurs to specific subunits. The hemocyanin of *A. leptodactylus* consists of four immunologically different subunits (α′, α, β, γ) with a stoichiometry of 2:2:4:4 [12]. Thus, it is tempting to assume, that one type of binding site corresponds to binding sites on subunit β and the other type on subunit γ. Both subunit types are exposed to the solvent and therefore easily accessible for the effectors. One of the subunits does not discriminate between urate and caffeine, the binding affinity is similar. The other subunits preferentially bind urate. The different binding affinity for the low affinity-sites for urate and caffeine cannot be of steric origin. One might consider that the two sites are located close to each other at the interface between β and γ subunit and that binding of the first influences binding of the second. This would correspond to a model of 4 independent dimers which display cooperativity. However, this type of model was excluded based on the results of the displacement experiments.

The stoichiometry might be checked by investigating the binding of the effectors to *Astacus* hemocyanin dissociated into subunits. However, these are difficult to obtain without damage, which is likely to reduce the binding affinity of the effectors. Furthermore, the binding constant and binding enthalpy for isolated subunits cannot be expected to agree with those for the intact 12-mer. The modulation of the oxygen binding properties by urate shows, that binding is specific for certain conformations. The binding characteristics of the

effector are therefore coupled to the quaternary structure. Thus, no unambiguous binding parameters for the binding of effectors to isolated subunits can be obtained.

Whatever model is employed for the interpretation of the data, the experimental binding curves show, that caffeine binding is weaker (or involves less binding sites) than urate binding for hemocyanin from *A. leptodactylus*. This result is in marked contrast to the results for hemocyanin from *H. vulgaris*. For this species, a stoichiometry of two and a binding constant of 8500 M^{-1} was determined [24]. In contrast to *A. leptodactylus*, the binding of caffeine to this hemocyanin leads to stronger shifts in the oxygen binding curves [25] than urate. ITC-experiments reveal that the binding affinity of caffeine to oxy-hemocyanin is higher and cooperative binding has to be assumed [24]. Obviously, the very similar quaternary structure of these two hemocyanins does not imply that binding of effector occurs at the same binding sites. Furthermore, the specificity towards the chemical structure also seems to be species dependent, indicating differences in the detailed structure of the binding sites.

5.1. Physiological considerations

The urate concentration in the hemolymph of *A. leptodactylus* increases from 20 to 150 μM, when the animal is forced to leave its normal aqueous habitat [33]. Based on the binding constants given above for two types of sites at a total concentration of 20 μM urate the saturation level of hemocyanin can be calculated to be approximately 7%. In contrast, at 150 μM urate, the saturation level is approximately 52%. Thus, the saturation level will be regulated in vivo. A typical hemocyanin concentration in the hemolymph is 35 μM, which corresponds to 280 μM binding sites for urate. Thus, at both concentrations of urate, a large percentage of the urate molecules exist in the protein-bound form: at 20 μM it is 98.8%, at 150 μM urate it is still 97%. Thus, due to the large number of binding sites one might consider hemocyanin from *A. leptodactylus* both as an oxygen carrier and as an urate binding protein. When this calculation is performed for the other models discussed, the numbers are similar and therefore independent of the model.

6. Conclusion

Hemocyanin from *A. leptodactylus* offers two types of independent binding sites for urate and for its analogue caffeine. The two types of sites exhibit different specificity towards the chemical structure of the effector molecule. The value of the corresponding binding constants ensures that the degree of saturation with respect to the effector varies significantly in the range of urate concentration typically found in the hemolymph. Thus, a modulation of oxygen binding properties can be achieved by effector binding under these conditions. However, whether both binding sites are important for allosteric interaction is not clear. The location of these binding sites can only be hypothesized: possibly effector binding occurs to specific subunits in the $2\times$ hexameric structure.

From a more general point of view, this study shows that the use of an analogue to determine the stoichiometry of binding for a certain effector might be misleading. Additionally, our simulations for the nesting model showed, that a binding process exhibiting weak cooperativity might result in binding curves, which look like binding of n identical binding sites. However, the apparent stoichiometry obtained by such an analysis is significantly lower than the actual stoichiometry. Although it was not necessary to assume cooperative binding in this particular case, it might be useful to be considered in other experiments.

We also showed that an apparent dependence of binding parameters on protein concentration might be an indication of such a weak, hidden cooperativity, as shown for data simulated in terms of the MWC-model. A similar behaviour can be found in the work of Terada et al. [34], where the binding of nucleotides to GroEL was investigated by ITC.

Acknowledgements

This work was granted by the NMFZ, Mainz.

Appendix A

The different binding models are introduced in terms of their binding polynomials P. For a given binding polynomial the fraction of occupied binding sites $\bar{x}$ is yielded by

$$\bar{x} = \frac{\partial \ln P}{n \partial \ln x}$$

where x is the free ligand concentration and n the number of binding sites per oligomer. The concentration of bound effector is then given by

$$c_{\text{bound}} = n\bar{x}[\text{Hc}]_o$$

where $[\text{Hc}]_o$ is the total hemocyanin concentration. If the binding polynomial includes more than one binding process, each binding process is characterized by a binding constant $K_{m,}$ the stoichiometry n_m and the corresponding binding enthalpy ΔH_m. Thus, in order to set up the equations for the reaction enthalpy, one has to calculate the concentration of bound ligand for each of these binding processes. The fraction of occupied binding sites which are involved in a certain binding process described by K_m can be obtained from the binding polynomial as follows:

$$\bar{x}_m = \frac{\partial \ln P}{n_m \partial \ln K_m} \tag{A1}$$

The total reaction enthalpy is then obtained as the sum of the contributions of the different processes

$$\Delta H = \left(\sum_{m=1}^{N_m} \Delta H_m \bar{x}_m n_m \right) [\text{Hc}]_o V_o \tag{A2}$$

The equations for ΔH given in this section describe the reaction enthalpy evolving after titrating a certain amount of ligand to ligand-free hemocyanin solution. Thus, they correspond to ΔH_i for the i-th titration step in an ITC experiment.

For those models, which were also applied to the competition experiments between urate and caffeine, the binding polynomial in presence of both effectors is given. Eq. (A2) is then still applicable. In these cases x_u represents the free urate concentration, whereas x_c denotes the free caffeine concentration. The corresponding binding constants for each individual effector is indexed with 'u' for urate and 'c' for caffeine.

A.1. Model 1: n identical binding sites including unspecific binding

This model is a special case of a binding process involving two types of binding sites, characterized by the binding constants K_{sp} and K^{mic}, and the stoichiometries n and n_{unsp}. The binding polynomial for such a process is

$$P = (1 + K_{sp}x)^n (1 + K^{mic}x)^{n_{unsp}}$$

Unspecific binding is characterized by a low binding constant K^{mic}. Then, $K^{mic}x \ll 1$ and one may set

$$(1 + K^{mic}x)^{n_{unsp}} \approx 1 + n_{unsp}K^{mic}x := 1 + K_{unsp}x$$
$$\Rightarrow P = (1 + K_{sp}x)^n (1 + K_{unsp}x)$$

Thus, for $x < 500$ μM, the above approximation is valid for binding constants $K_{unsp} < 300\ \text{M}^{-1}$ (deviation < 1%). According to Eq. (A1), the concentration of effector molecules bound to specific binding sites is given by

$$c_{sp} = \frac{\partial \ln P}{n \partial \ln K_{sp}} n[\text{Hc}]_o = \frac{xK_{sp}}{1 + xK_{sp}} n[\text{Hc}]_o$$

The concentration of effector molecules bound to the unspecific binding sites is given by

$$c_{unsp} = \frac{\partial \ln P}{\partial \ln K_{unsp}} [\text{Hc}]_o = xK_{unsp}[\text{Hc}]_o$$

Obeying mass conservation $c_{tot} = c_{unsp} + c_{sp} + x$, the free effector concentration can be calculated to be

$$x = \left(\left(\frac{[\text{Hc}]_o(K_{sp}n + K_{unsp}) + 1 - c_{tot}K_{sp}}{2K_{sp}([\text{Hc}]_o K_{unsp} + 1)} \right)^2 \right.$$

$$+\frac{c_{\mathrm{tot}}}{K_{\mathrm{sp}}([\mathrm{Hc}]_{\mathrm{o}}K_{\mathrm{unsp}}+1)}\Bigg)^{1/2}$$

$$-\frac{[\mathrm{Hc}]_{\mathrm{o}}(K_{\mathrm{sp}}n+K_{\mathrm{unsp}})+1-c_{\mathrm{tot}}K_{\mathrm{sp}}}{2K_{\mathrm{sp}}([\mathrm{Hc}]_{\mathrm{o}}K_{\mathrm{unsp}}+1)}$$

According to Eq. (A2) an analytical expression for the reaction enthalpy can be obtained as a function of total ligand and total hemocyanin concentration (c_{tot} and $[\mathrm{Hc}]_{\mathrm{o}}$), based on the following equation

$$\Delta H_{\mathrm{i}}=(\Delta H^{\mathrm{o}}_{\mathrm{sp}}c_{\mathrm{sp}}+\Delta H^{\mathrm{o}}_{\mathrm{unsp}}c_{\mathrm{unsp}})V_{\mathrm{o}} \tag{A3}$$

by using the equations above for c_{sp}, c_{unsp} and x.

The unspecific binding contributes only little to the observed binding curve. The two parameters describing unspecific binding (K_{unsp}, ΔH_{unsp}) are strongly correlated in the fitting process. Therefore, the value for K_{unsp} was kept constant ($K_{\mathrm{unsp}}=10\ \mathrm{M}^{-1}$). The choice of this value has no significant influence on the values of the parameters describing the specific binding process (K, n and ΔH) as long as $K_{\mathrm{unsp}}<300\ \mathrm{M}^{-1}$. This was checked by a series of fits, were K_{unsp} was varied (results not shown). The corresponding values for ΔH_{unsp} change roughly reciprocal with changes in K_{unsp}, reflecting the above mentioned strong correlation between the two parameters.

A.2. Model 2: stacking model

The stacking model assumes, that two effector molecules can bind at each of the n binding sites on the hemocyanin molecule. The binding constant for the first effector is denoted by b_1, the binding constant for the second one by D_{stack}. The latter can be regarded as stacking of two effector molecules at the binding site. We assume, that no mixed dimers may exist.

The binding polynomial P_{stack} for stacking on the binding site is given by

$$P_{\mathrm{stack}}=P_{\mathrm{o}}^{n}$$

$$P_{\mathrm{o}}=(1+b_1^{\mathrm{u}}x_{\mathrm{u}}(1+D^{\mathrm{u}}_{\mathrm{stack}}x_{\mathrm{u}})$$

$$+b_1^{\mathrm{c}}x_{\mathrm{c}}(1+D^{\mathrm{c}}_{\mathrm{stack}}x_{\mathrm{c}}))$$

$$=(1+b_1^{\mathrm{u}}x_{\mathrm{u}}+D^{\mathrm{u}}_{\mathrm{stack}}b_1^{\mathrm{u}}x_{\mathrm{u}}^2+b_1^{\mathrm{c}}x_{\mathrm{c}}+D^{\mathrm{c}}_{\mathrm{stack}}b_1^{\mathrm{c}}x_{\mathrm{c}}^2)$$

The concentration of effector molecules bound in the first step is given by

$$c_{\mathrm{mon}}(a)=\frac{\partial\ln P}{n\partial\ln b_1^{\mathrm{a}}}=\frac{b_1^{\mathrm{a}}x_{\mathrm{a}}+D^{\mathrm{a}}_{\mathrm{stack}}b_1^{\mathrm{a}}x_{\mathrm{a}}^2}{P}n[\mathrm{Hc}]_{\mathrm{o}}$$

$$a=u,\ c$$

The concentration of effector molecules bound in the second step (stacking on the binding site) is given by

$$c_{\mathrm{stack}}(a)=\frac{\partial\ln P}{n\partial\ln D^{\mathrm{a}}_{\mathrm{stack}}}=\frac{D^{\mathrm{a}}_{\mathrm{stack}}b_1^{\mathrm{a}}x_{\mathrm{a}}^2}{P}n[\mathrm{Hc}]_{\mathrm{o}}$$

$$a=u,\ c$$

Thus, for the reaction enthalpy one obtains

$$\Delta H_{\mathrm{i}}=[\Delta H^{\mathrm{o,u}}_{\mathrm{mon}}c_{\mathrm{mon}}(u)+\Delta H^{\mathrm{o,u}}_{\mathrm{stack}}c_{\mathrm{stack}}(u)$$

$$+\Delta H^{\mathrm{o,c}}_{\mathrm{mon}}c_{\mathrm{mon}}(c)+\Delta H^{\mathrm{o,c}}_{\mathrm{stack}}c_{\mathrm{stack}}(c)]V_{\mathrm{o}} \tag{A4}$$

A.3. Model 3: two types of sites

In this model two types of independent binding sites are assumed, described by the binding constants t_1 and t_2. Type one contains n_1 binding sites, type two n_2 binding sites. The binding polynomial P_{two} is given by

$$P_{\mathrm{two}}=P_1^{n_1}P_2^{n_2}$$

$$P_1=1+t_1^{\mathrm{u}}x_{\mathrm{u}}+t_1^{\mathrm{c}}x_{\mathrm{c}}\quad P_2=1+t_2^{\mathrm{u}}x_{\mathrm{u}}+t_2^{\mathrm{c}}x_{\mathrm{c}}$$

The concentration of urate ($a=u$) and caffeine ($a=c$) molecules bound to the first ($i=1$) or the second ($i=2$) binding site is given by

$$c_{\mathrm{ti}}(a)=\frac{\partial\ln\mathrm{P}}{n_{\mathrm{i}}\partial\ln t_{\mathrm{i}}^{\mathrm{a}}}=\frac{t_{\mathrm{i}}^{\mathrm{a}}x_{\mathrm{a}}}{P_{\mathrm{i}}}n[\mathrm{Hc}]_{\mathrm{o}}\quad a=u,c$$

$$i=1,2$$

For the binding sites analyzed here, we set

$n_1 = n_2 = n$. Thus, for the reaction enthalpy one obtains

$$\Delta H_i = [\Delta H_{t1}^{o,u} c_{t1}(u) + \Delta H_{t2}^{o,u} c_{t2}(u) + \Delta H_{t1}^{o,c} c_{t1}(c) + \Delta H_{t2}^{o,c} c_{t2}(c)] V_o \quad \text{(A5)}$$

A.4. Model 4: nesting model

The nesting model describes the interaction of two allosteric units composing the native protein in a hierarchical manner. Each allosteric unit behaves according to the MWC model. The binding polynomial for the nesting model of a 2×6-mer with m effector binding sites per hexamer is given by [5]

$$P = (P_{rR}^6 Q_{rR}^m + l_R P_{tR}^6 Q_{tR}^m)^2 + L(P_{rT}^6 Q_{rT}^m + l_T P_{tT}^6 Q_{tT}^m)^2$$

where $P_{\alpha\beta} = 1 + z_{\alpha\beta} u$ is the bonding of oxygen u, $Q_{\alpha\beta} = 1 + K_{\alpha\beta} x$ is the binding of effector x, and $\alpha\beta$ = tT, rT, tR, rR.

The equilibrium between the four conformations rR, rT, tR, tT is given by the allosteric equilibrium constants L, l_R and l_T. Two conformations, rR and rT, with high oxygen affinities exist. Furthermore, urate and caffeine stabilize conformations present under oxygenated conditions, since the p_{50} is shifted towards lower values [13,15–17]. Therefore, under high oxygen concentrations we can neglect the low affinity conformations tT and tR. Thus, the binding polynomial for binding of the effector is essentially a MWC-type binding polynomial. The binding polynomial for the analysis of the ITC experiments is therefore ($n = 2m$).

$$Q = P_{rR}^{12} Q_{rR}^n + L P_{rT}^{12} Q_{rT}^n \quad \text{(A6)}$$

The binding polynomial for the allosteric units in presence of urate and caffeine is given by

$$Q_{\alpha\beta} = 1 + K_{\alpha\beta}^u x_u + K_{\alpha\beta}^c x_c \quad \alpha\beta = rR, rT$$

The concentration of effector bound to binding sites in conformation rR is given by

$$c_{rR}(a) = \frac{\partial \ln P}{n \partial \ln K_{rR}^a} n[\mathrm{Hc}]_o = \frac{x_a K_{rR}^a P_{rR}^{12} Q_{rR}^{n-1}}{P} n[\mathrm{Hc}]_o = \frac{x_a K_{rR}^a Q_{rR}^{n-1}}{P(L_o)} n[\mathrm{Hc}]_o$$

Here, L is substituted in the binding polynomial P by the following transformed allosteric equilibrium constants

$$L_o = L \frac{P_{rT}^{12}}{P_{rR}^{12}}$$

The concentration of effector bound to binding sites in conformation rT is given by

$$c_{rT}(a) = \frac{\partial \ln P}{n \partial \ln K_{rT}^a} n[\mathrm{Hc}]_o = \frac{x_a L_o K_{rT}^a Q_{rT}^{n-1}}{P(L_o)} n[\mathrm{Hc}]_o$$

The concentration of protein molecules in the conformation rR is given by

$$M_{rR} = \frac{Q_{rR}^{12}}{Q_{rR}^{12} + L_o Q_{rT}^{12}} [\mathrm{Hc}]_o$$

In absence of effector, this simplifies to

$$M_{rR}^o = \frac{1}{1 + L_o} [\mathrm{Hc}]_o$$

Upon addition of effector molecules to the hemocyanin solution not only bound effector has to be considered but also the conformational distribution which is shifted compared to the situation in absence of effectors. The contribution of reaction enthalpy due to the conformational change occurring upon effector binding can be entirely expressed in terms of M_{rR} due to mass conservation. Thus, the reaction enthalpy is given by

$$\Delta H_i = [\Delta H_{rR}^{o,u} c_{rR1}(u) + \Delta H_{rT}^{o,u} c_{tT}(u)$$

$$+\Delta H_{\mathrm{rR}}^{\mathrm{o,c}} c_{\mathrm{rR}}(c) + \Delta H_{\mathrm{rT}}^{\mathrm{o,c}} c_{\mathrm{rT}}(c) + \Delta H_{\mathrm{conf}}(M_{\mathrm{rR}} - M_{\mathrm{rR}}^{\mathrm{o}})]V_{\mathrm{o}} \quad \text{(A7)}$$

Here, the value of ΔH_{conf} corresponds to the enthalpy-difference between the rR and the rT conformation of the fully oxygenated molecule. The enthalpy contribution from the conformational change (ΔH_{conf}) does not simply parallel effector binding to conformation rR or rT. In order to show this, ΔH_{i} for the case that only one effector (urate) is present, is given in more detail:

$$\begin{aligned}
\Delta H_{\mathrm{i}} &= [\Delta H_{\mathrm{rR}}^{\mathrm{o,u}} c_{\mathrm{rR}1}(u) + \Delta H_{\mathrm{rT}}^{\mathrm{o,u}} c_{\mathrm{tT}}(u) \\
&\quad + \Delta H_{\mathrm{conf}}(M_{\mathrm{rR}} - M_{\mathrm{rR}}^{\mathrm{o}})]V_{\mathrm{o}} \\
&= \Bigg[\Delta H_{\mathrm{rR}}^{\mathrm{o,u}} K_{\mathrm{rR}} x_{\mathrm{u}} Q_{\mathrm{rR}}^{n-1} \\
&\quad + L_{\mathrm{o}} \Delta H_{\mathrm{rT}}^{\mathrm{o,u}} K_{\mathrm{rR}} x_{\mathrm{u}} Q_{\mathrm{rT}}^{n-1} \\
&\quad + \Delta H_{\mathrm{conf}} \frac{L_{\mathrm{o}}}{1+L_{\mathrm{o}}} (Q_{\mathrm{rR}}^{n} - Q_{\mathrm{tR}}^{n}) \Bigg] \frac{n[\mathrm{Hc}]_{\mathrm{o}} V_{\mathrm{o}}}{P(L_{\mathrm{o}})} \\
&= \Bigg[\left(\Delta H_{\mathrm{rR}}^{\mathrm{o,u}} + \Delta H_{\mathrm{conf}} \frac{L_{\mathrm{o}}}{1+L_{\mathrm{o}}} \right) K_{\mathrm{rR}} x_{\mathrm{u}} Q_{\mathrm{rR}}^{n-1} \\
&\quad + \left(L_{\mathrm{o}} \Delta H_{\mathrm{rT}}^{\mathrm{o,u}} - \Delta H_{\mathrm{conf}} \frac{L_{\mathrm{o}}}{1+L_{\mathrm{o}}} \right) K_{\mathrm{rT}} x_{\mathrm{u}} Q_{\mathrm{rT}}^{n-1} \\
&\quad + \Delta H_{\mathrm{conf}} \frac{L_{\mathrm{o}}}{1+L_{\mathrm{o}}} (Q_{\mathrm{rR}}^{n-1} - Q_{\mathrm{rT}}^{n-1}) \Bigg] \\
&\quad \times \frac{n[\mathrm{Hc}]_{\mathrm{o}} V_{\mathrm{o}}}{P(L_{\mathrm{o}})}
\end{aligned}$$

The last term in the bracket cannot be treated as a mere change in the absolute value of ΔH_{rR} or ΔH_{rT}. Thus, an extra term is needed. In order to fit the equation to the data, this equation, which is an polynomial of n-th order in x_{u} has to be solved for x_{u}. Since no general solution exists, the values of the parameters K_{rR}, K_{rT}, ΔH_{rT}, ΔH_{rR} and ΔH_{conf} were estimated in a two-step, iterative process as described under Section 3.

A.5. Model 5: interacting sites

Assume a model of n pairs of interacting binding sites. The interaction might for example be of sterical origin when the binding sites are located close to each other. These pairs are independent from each other; cooperative interactions occur only between the two binding sites of each pair, and is described by the binding constants K_1 and K_2. The binding polynomial for n pairs of two interacting sites is given by

$$P_{\mathrm{dim},n} = P_{\mathrm{dim}}^{n}$$

$$P_{\mathrm{dim}} = \left(1 + 2K_1^{\mathrm{u}} x_{\mathrm{u}} \left(1 + \frac{K_2^{\mathrm{u}} x_{\mathrm{u}} + K_2^{\mathrm{c}} x_{\mathrm{c}}}{2} \right) + 2K_1^{\mathrm{c}} x_{\mathrm{c}} \left(1 + \frac{K_2^{\mathrm{u}} x_{\mathrm{u}} + K_2^{\mathrm{c}} x_{\mathrm{c}}}{2} \right) \right)$$

The concentration of effector molecules bound to the first site is given by

$$\begin{aligned}
c_1(a) &= \frac{\partial \ln P}{n \partial \ln K_1^a} \\
&= \frac{K_1^a x_a + K_2^a K_1^a x_a^2 + K_2^b K_1^a x_a x_b}{P} n[\mathrm{Hc}]_{\mathrm{o}} \\
a &= \mathrm{u}, \mathrm{c} \quad b = \mathrm{c}, \mathrm{u} \neq a
\end{aligned}$$

The concentration of effector molecules bound in the second step (stacking on the binding site) is given by:

$$\begin{aligned}
c_2(a) &= \frac{\partial \ln P}{n \partial \ln K_2^a} = \frac{K_2^a K_1^a x_a^2 + K_2^a K_1^b x_a x_b}{P} n \\
&\times [\mathrm{Hc}]_{\mathrm{o}} \quad a = \mathrm{u},\mathrm{c} \quad b = \mathrm{u}, \mathrm{c} \neq a
\end{aligned}$$

Thus, for the reaction enthalpy one obtains

$$\Delta H_{\mathrm{i}} = [\Delta H_1^{\mathrm{o,u}} c_1(u) + \Delta H_2^{\mathrm{o,u}} c_2(u) + \Delta H_1^{\mathrm{o,c}} c_1(c) + \Delta H_2^{\mathrm{o,c}} c_2(c)]V_{\mathrm{o}} \quad \text{(A8)}$$

Here it is assumed, that the binding affinity for the second site is independent of the type of effector bound to the first site. This is probably an overestimation for the binding of urate in presence of caffeine. However, even then the simulated binding curve for titration of urate in presence of caffeine predicts weaker binding than observed in the experiment.

From this model the binding parameters for the stacking model for the binding curves of each

single effector were deduced since for the latter no fitting routine was implemented. The re-interpretation of the fitting parameters was done based on comparison of Eq. (A8) and Eq. (A4) together with c_{mon}, c_{stack} and c_1, c_2, respectively. The comparison yields the relations given after Eq. (4) in Section 3.

References

[1] B. Salvato, M. Beltramini, Hemocyanins: molecular architecture, structure and reactivity of the binuclear copper site, Life Chem. Rep. 8 (1990) 1–47.

[2] J. Markl, H. Decker, Molecular structure of arthropod hemocyanins, Adv. Comp. Environ. Physiol. 13 (1992) 325–376.

[3] K.E. van Holde, K.A. Miller, Hemocyanins, Adv. Protein Chem. 47 (1995) 1–81.

[4] H.D. Ellerton, N.F. Ellerton, H.A. Robinson, Hemocyanin — a current perspective, Prog. Biophys. Mol. Biol. 41 (1983) 143–248.

[5] C.H. Robert, H. Decker, B. Richey, S.J. Gill, J. Wyman, Nesting: hierarchies of allosteric interaction, Proc. Natl. Acad. Sci. USA 84 (1987) 1891–1895.

[6] H. Decker, R. Sterner, Nested allostery of arthropodan hemocyanin (*Eurypelma californicum* and *Homarus vulgaris*), J. Mol. Biol. 211 (1990) 281–293.

[7] K.A. Magnus, B. Hazes, H. Ton-That, C. Bonaventura, J. Bonaventura, W.G.J. Hol, Crystallographic analysis of oxygenated and deoxygenated states of arthropod hemocyanin shows unusual differences, Proteins 19 (1994) 302–309.

[8] B. Hazes, K.A. Magnus, C. Bonaventura et al., Crystal structure of deoxygenated *Limulus polyphemus* subunit II hemocyanin at 2.18 Å resolution: clues for a mechanism for allosteric regulation, Protein Sci. 2 (1993) 597–619.

[9] W.P. Gaykema, A. Volbeda, W.G.J. Hol, Structure determination of *Panulirus interruptus* haemocyanin at 3.2 Å resolution, J. Mol. Biol. 197 (1986) 255–275.

[10] A. Volbeda, W.G.J. Hol, Crystal structure of hexameric haemocyanin from *Panulirus interruptus* refined at 3.2 Å resolution, J. Mol. Biol. 209 (1989) 249–279.

[11] M.van Heel, P. Dube, Quaternary structure of multihexameric arthropod hemocyanins, Micron 25 (1994) 387–418.

[12] W. Stöcker, U. Raeder, M.M. Bijolt, T. Wichertjes, E.F.J. van Bruggen, J. Markl, The quaternary structure of four crustacean two-hexameric hemocyanins: immunocorrelation, stoichiometry, reassembly and topology of individual subunits, J. Comp. Physiol. B 158 (1988) 271–289.

[13] J.P. Truchot, F.H. Lallier, Modulation of the oxygen-carrying function of hemocyanin in crustaceans, News Physiol. Sci. 7 (1992) 49–52.

[14] J.P. Truchot, Lactate increases the oxygen affinity of crab hemocyanin, J. Exp. Zool. 214 (1980) 205–208.

[15] S. Morris, C.R. Bridges, M.K. Grieshaber, A new role for uric acid: modulator of haemocyanin oxygen affinity in crustaceans, J. Exp. Zool. 235 (1985) 135–139.

[16] F. Lallier, J.P. Truchot, Hemolymph oxygen transport during environmental hypoxia in the shore crab, *Carcinus maenas*, Respir. Physiol. 77 (1989) 323–336.

[17] S. Morris, C.R. Bridges, M.K. Grieshaber, The potentiating effect of purine bases and some of their derivatives on the oxygen affinity of haemocyanin from the crayfish *Austropotamobius pallipes*, J. Comp. Physiol. B 156 (1986) 431–440.

[18] S. Morris, Organic ions as modulators of respiratory pigment function during stress, Physiol. Zool. 63 (1990) 253–287.

[19] S. Morris, B.R. McMahon, Potentation of hemocyanin oxygen affinity by catecholamines in the crab *Cancer magister*: a specific effect of dopamin, Physiol. Zool. 62 (1989) 654–667.

[20] N.K. Sanders, J.J. Childress, Specifc effects of thiosulfate and L-lactate on hemocyanin-O_2 affinity in a brachyuran hydrothermal crab, Mar. Biol. 113 (1992) 175–180.

[21] B.A. Johnson, C. Bonaventura, J. Bonaventura, Allostery in *Callinectes sapidus* hemocyanin: cooperative oxygen binding and interactions with L-lactate, calcium, and protons, Biochemistry 27 (1988) 1995–2001.

[22] F. Arisaka, K.E. van Holde, Allosteric properties and the association equilibria of hemocyanin from *Callianassa californiensis*, J. Mol. Biol. 134 (1979) 41–73.

[23] M. Brouwer, B. Serigstad, Allosteric control in *Limulus polyphemus* hemocyanin: functional relevance of interactions between hexamers, Biochem. J. 28 (1989) 8819–8827.

[24] M. Menze, N. Hellmann, H. Decker, M. Grieshaber, Binding of urate and caffeine to haemocyanin of the lobster *Homarus vulgaris* (E.) studied by isothermal titration calorimetry, Biochemistry 39 (2000) 10806–10811.

[25] A. Nies, B. Zeis, C.R. Bridges, M.K. Grieshaber, Allosteric modulation of haemocyanin oxygen-affinity by L-lactate and urate in the lobster *Homarus vulgaris*. II. Characterization of specific effector binding sites, J. Exp. Biol. 168 (1992) 111–124.

[26] P. Scheibe, E. Bernt, H.U. Bergmeyer, Methoden der enzymatischen Analyse, Verlag Chemie, Weinheim, Germany, 1974.

[27] T. Wiseman, S. Williston, J.F. Brandts, L.N. Lin, Rapid measurement of binding constants and heats of binding using a new titration calorimeter, Anal. Biochem. 179 (1989) 131–137.

[28] E. Freire, O.L. Mayorga, M. Straume, Isothermal titration calorimetry, Anal. Chem. 62 (1990) 949b–950a.

[29] J.E. Ladbury, B.Z. Chowdry, Sensing the heat-the application of Isothermal Titration Calorimetry to thermody-

namic studies of biomolecular interactions, Chem. Biol. 3 (1996) 791–801.
[30] H. Fritzsche, I. Petri, H. Schutz, K. Weller, P. Sedmera, H. Lang, On the interaction of caffeine with nucleid acids. III, Biophys. Chem. 11 (1980) 109–119.
[31] A.J. Dykens, Purineolytic capacity and origin of hemolymph urate in *Carcinus maenas* during hypoxia, Comp. Biochem. Physiol. B 98 (1991) 579–582.
[32] M.F. Perutz, G. Fermi, D.J. Abrahan, C. Poyart, E. Bursaux, Hemoglobin as a receptor of drugs and peptides: X-ray studies of the stereochemistry of binding, J. Am. Chem. Soc. 108 (1986) 1064–1078.
[33] H.M. Czytrich, C.R. Bridges, M. Grieshaber, Purinstoffwechsel von *Astacus leptodactylus*, Verh. Deut. Zool. Ges. 80 (1987) 207.
[34] T.P. Terada, K. Kuwajima, Thermodynamics of nucleotide binding to the chaperonin GroEL studies by isothermal titration calorimetry: evidence for non-cooperative nucleotide binding, Biochim. Biophys. Acta 1421 (1999) 269–281.